Journal of Applied Polymer Science

Synthesis and Drug-Release Studies of Low-Fouling Zwitterionic Hydrogels with Enhanced Mechanical Strength

Renchang Zeng, Jiang Cheng, Shouping Xu, Qin Liu, Xiufang Wen, Pihui Pi

College of Chemistry and Chemical Engineering, South China University of Technology, Guangzhou 510640, People's Republic of China

Correspondence to: S. Xu (E-mail: cespxu@scut.edu.cn)

ABSTRACT: Reversible addition–fragmentation chain-transfer polymerization was introduced to prepare a series of zwitterionic poly(-hydroxyethyl methacrylate)-*g*-poly(sulfobetaine methacrylate) (PSBMA) hydrogels (HSGs) with different monomer feed ratios. Compared with PSBMA hydrogels, these hydrogels exhibited enhanced mechanical strengths. Then, the HSGs were characterized by Fourier transform infrared spectroscopy, scanning electron microscopy, and swelling measurements. We found that the equilibrium swelling ratios, mechanical strengths, and drug-release behaviors were significantly affected by the feed ratios of the gels. The hydrophilic tetracycline hydrochloride release results suggest that the hydrophilic drug release from the HSGs could be prolonged by the variation of the hydroxyethyl methacrylate amount in the gel networks. The bovine serum albumin adsorption data showed that the zwitterionic HSG with 18.2 wt % sulfobetaine methacrylate exhibited good protein-resistance properties. © 2014 Wiley Periodicals, Inc. J. Appl. Polym. Sci. **2014**, *131*, 41041.

KEYWORDS: biomaterials; drug-delivery systems; gels; mechanical properties

Received 24 February 2014; accepted 17 May 2014

DOI: 10.1002/app.41041

INTRODUCTION

Hydrogels, three-dimensional polymeric networks with some excellent properties, such as a high water content and a sensitivity to stimuli, have been widely applied in pharmaceutical, biomedical, and industrial fields. Great attention has been focused on the applications of hydrogels in controlled drug-release systems to provide a sustained therapeutic level of targeted drug concentration.[1,2] When used as a drug-release device, hydrogels may suffer from protein fouling on the hydrogel surface; this would probably trigger an immune response and inflammation[3] and lead to the removal of the hydrogel. A polysulfobetaine-based hydrogel was found to show high protein-resistance abilities because of the formation of a hydration layer between the hydrogel surface and protein molecules via electrostatic interaction and hydrogen bonding.[4] So, it is possible to fabricate low-protein fouling hydrogels with sulfobetaine methacrylate (SBMA). However, we found that polysulfobetaine-based hydrogels turned out to be very brittle in the fully swollen state; this will limit its applications in drug-delivery devices where a high mechanical strength is required. The low mechanical strength of the swollen gel was mainly caused by the weak intermolecular interactions and loose polymeric networks.[5,6] Furthermore, the relaxed gel networks produced a low-density region on the surface of the hydrogel; this allowed the drug molecules to diffuse out from the hydrogel matrix easily and, hence, made the hydrogel fail to achieve sustained release for a long time.[7]

Recently, several strategies have been proposed to overcome the low strength of the swollen gel; these have included the design of an interpenetrating polymer network,[8] the construction of a double network,[9] the use of organic/inorganic hybrids,[10,11] and the incorporation of intermolecular interactions.[6,12] Among these strategies, the incorporation of intermolecular interactions was an effective and feasible method for improving the mechanical strength. For example, Tang et al.[12] prepared a high-strength hydrogel with thermal sensitivity with *N*-isopropyl acrylamide and 2-vinyl-4,6-diamino-1,3,5-triazine; the improved mechanical strength of this gel was attributed to the hydrogen-bonding interactions of 2-vinyl-4,6-diamino-1,3,5-triazine through the formation of six-membered ring structure. Bostan et al.[13] developed a poly(hydroxyethyl methacrylate) (PHEMA)-based hydrogel by copolymerization with acrylic acid; it exhibited similar mechanical and tribological properties with articular cartilage, probably because of the pressurization of molecular water and charged ions. Hydroxyethyl methacrylate (HEMA) is a chemically stable and biocompatible monomer that bears hydroxyl groups; it is known that HEMA is able to form complementary hydrogen bonding to improve intermolecular interactions via hydroxyl groups. Thus, it was anticipated that the introduction of HEMA

Table I. Feed Compositions and Sample Codes for the Grafted Hydrogels

	Polymer code			
Composition	HG0	HSG10	HSG18	HSG25
SBMA (wt %)	0	10.8	18.2	25.8
HEMA (wt %)	100	89.2	81.8	74.2
MBA (g)	0.08	0.08	0.08	0.08
TTC (mg)	5	5	5	5
H2O (mL)	7	7	7	7

The weight of the total monomer used for polymerization was 3.0 g. The contents of APS and TEMED were 0.01 g and 0.1 mL, respectively.

into a polymeric network could improve the mechanical properties of polysulfobetaine-based hydrogels. To date, reports on the preparation of low-fouling and high-strength hydrogels based on SBMA and HEMA have been limited.

In this study, a series of zwitterionic PHEMA-*g*-poly(sulfobetaine methacrylate) (PSBMA) hydrogels (HSGs) was synthesized by aqueous reversible addition–fragmentation chain-transfer (RAFT) polymerization with SBMA and HEMA as monomers. RAFT polymerization is a controlled/ living free-radical polymerization method usually used for the synthesis of well-defined polymers.[14,15] As far as we know, few studies have been reported on the preparation of hydrogels with RAFT polymerization.[4,16–18] The aim of this research was to synthesize a low-fouling and high-strength hydrogel via the RAFT polymerization technique and to investigate the effects of the feed ratio on the properties of the resulting hydrogels, such as the mechanical strength, swelling ratio (SR), and drug-release rate. The chemical compositions and morphologies were characterized by Fourier transform infrared (FTIR) spectroscopy and scanning electron microscopy (SEM). Tetracycline hydrochloride (TCHC) was selected as a model drug to study the drug-release kinetics of these hydrogels with various feed ratios. Finally, the antifouling properties of the HSGs with certain contents of sulfobetaine monomer were investigated and compared with those of the PHEMA hydrogel (HG).

EXPERIMENTAL

Materials

2-hydroxyethyl methacrylate (HEMA), *N,N′*-methylene bisacrylamide (MBA), ethyl ether, ammonium persulfate (APS), *N,N,N′,N′*-tetramethylethylenediamine (TEMED), bovine serum albumin (BSA), and Coomassie Brilliant Blue G-250 were purchased from Aladdin Chemicals (Shanghai, China). Phosphate-buffered saline (PBS) and TCHC were obtained from Amresco. *N*-(3-Sulfopropyl)-*N*-(methacryloxyethyl)-*N,N′*-dimethylammonium betaine (SBMA) was further purified by dissolution and recrystallization in ethanol. 2-(2-Carboxyethylsulfanylthiocarbonyl sulfanyl)propionic acid (TTC) was synthesized via a previously published method.[19]

Synthesis of the Hydrogels

For the synthesis of the grafted hydrogels, various feed ratios of HEMA/SBMA, APS (0.01 g), MBA (0.08 g), and TTC (0.005 g) were dissolved in 7.0 mL of distilled water, and then, the mixture was added to a polymerization tube with magnetic stirring. After three freeze–pump–thaw cycles, TEMED (0.1 mL) was added to facilitate gel formation. The tube polymerization was performed at 50°C for 24 h to produce the HSGs. This reaction procedure with the same monomer weight was also used for the preparation of the HEMA hydrogel. The obtained hydrogels were immersed in deionized water for 48 h to extract unreacted chemicals. These hydrogels were cut into small disks (12 mm in diameter and 3 mm in thickness) for further study. The feed compositions and polymer codes of the grafted hydrogels are presented in Table I. The numerals following HG and HSG show the approximate weight percentage of SBMA in the total monomer feeds. For instance, HSG18 represents an HSG with 18.2 wt % SBMA and 81.8 wt % HEMA.

Mechanical Strengths of the Hydrogels

The mechanical properties of the hydrogels were measured according to a previously reported method[20] with an Instron 3367 mechanical tester with a 20-kN load cell (Instron Corp.) at a 65% relative humidity. The swollen gel disk (12 mm in diameter and 3 mm in thickness) was placed on the center of a compression load cell and compressed to fragment at a constant rate of 2.0 mm/min.

Characterization of the Hydrogels

Before any characterization, the fully swollen hydrogels were dried in a vacuum freeze drier at −50°C for 24 h. The chemical compositions of the dried hydrogels were investigated with FTIR spectroscopy with a Bruker Vector 33 spectrophotometer in the range 4000–500 cm^{-1}. The morphologies of these hydrogels were visualized by SEM (HITACHI S-3700N) after the dried gels were coated with gold.

The SR of each hydrogel was studied by a gravimetric method at 25°C. The weight of the hydrogel was measured at a given time after surface water was wiped off with filter paper. SR was determined as follows:

$$\mathrm{SR} = (M_s - M_d)/M_d$$

where M_s is the mass of the swollen hydrogel at a certain temperature and M_d is the mass of the dry hydrogel.

In Vitro Drug Release from the Hydrogels

The freeze-dried hydrogels were immersed in a TCHC aqueous solution (10.0 mg/mL, 10 mL) at room temperature for 48 h to reach equilibrium. After equilibrium was reached, the excess water on the surfaces was wiped off, and these gels were placed at room temperature for 24 h and dried *in vacuo* for 48 h. The amount of TCHC entrapped by the hydrogel was determined by the weight of the dried drug-loaded hydrogel minus the weight of the dried gels.

We studied the average release amounts of these hydrogels by soaking the drug-entrapped hydrogels in 20 mL of deionized water for 72 h at 37°C. Then, an ultraviolet–visible spectrometer (Shimadzu UV-2450) was used to determine the concentration of the drug in the solution. The average release amount of the gel was calculated as follows:

$$\text{Average release amount} = W_{\mathrm{drug}}/W_{\mathrm{gel}}$$

where W_{drug} is the mass of drug released from the hydrogel, which could be calculated via the multiplication of the concentration of the drug solution by the volume of the solution, and W_{gel} is the mass of the dry hydrogel.

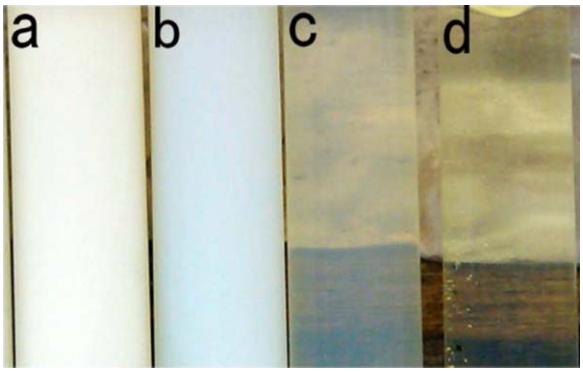

Figure 1. Photographs of (a) HG0, (b) HSG10, (c) HSG18, and (d) HSG25. [Color figure can be viewed in the online issue, which is available at wileyonlinelibrary.com.]

The *in vitro* drug-release behaviors were tested by the immersion of the drug-encapsulated hydrogels in 50 mL of deionized water at 25°C. At a predetermined time interval, 5.0 mL of the drug-release solution was removed for concentration measurement by a UV spectrophotometer at 357 nm and simultaneously replaced with 5.0 mL of fresh distilled water. The concentration of the drug-release solution was determined by a TCHC standard calibration curve. The drug-release results are shown in terms of the cumulative release amounts as a function of time. The cumulative release amount was determined as follows:

$$\text{Cumulative release amount} = M_t / M_0 \times 100\%$$

where M_t is the amount of drug in the release medium at a fixed time and M_0 is the amount of drug before release.

In Vitro Protein Adsorption Tests of the Hydrogels

The protein adsorption study method of the hydrogel was similar to a method previously reported by Li et al.[21] Briefly, the hydrogel disk (12 mm in diameter and 3 mm in thickness) was first rinsed with 20 mL PBS (pH 7.4) for 30 min. Then, the disk was soaked in 20 mL of 1.0 mg/mL BSA in PBS solution at 37°C. After 24 h, 1.0 mL of BSA solution was removed to a clean test tube; this was followed by the addition of 5.0 mL of coloring agent (Coomassie Brilliant Blue G-250). After incubation for 5 min, the protein concentration of the solutions was determined with a UV spectrometer (UV-2450, Shimadzu) at 595 nm. The calibration curve was preset by the measurement of the solutions with various protein concentrations. The protein adsorption ($\mu g/cm^2$) of the hydrogels was calculated as follows:

$$\text{Protein adsorption} = \frac{(C_0 - C_t)V}{A}$$

where C_0 and C_t are the BSA concentrations before and after the soaking of the hydrogel in the BSA solutions (mg/mL), respectively; V is the volume of the solution; and A is the effective surface area of the hydrogel (cm^2).

RESULTS AND DISCUSSION

Synthesis and Characterization of the Hydrogels

As shown in Figure 1, the transparency of the HSGs decreased with increasing HEMA content, and the pure PHEMA hydrogel (HG0) containing no SBMA was opaque. We concluded that the transparency of the gel was greatly affected by the presence of HEMA in the hydrogel; this was similar to the influence of the *N*-isopropylacrylamide content on the transparency of the poly(*N*-isopropylacrylamide-*co*-dimethyl aminoethyl methacrylate sulfate) hydrogel.[22] Usually, the opaque appearance is mainly caused by the heterogeneous structure of the gel. As a nonionic monomer, HEMA cannot be ionized by water molecules in the reaction medium; this would lead to the formation of hydrophobic microaggregates in the polymer structure and, hence, generate the heterogeneous gel network.[22,23] That is the reason why HG0 was opaque. On the other hand, SBMA is a hydrophilic monomer with anionic and cationic moieties; it can be ionized well and presents free ions solvated by water molecules; this is favorable for the reduction of the hydrophobic microaggregates and prevents the formation of microheterogeneity in the structure.[23] As a result, when the amount of zwitterionic SBMA was increased, the structural microhomogeneity increased accordingly, and the hydrogels tended to become transparent when the weight percentage of SBMA was increased to 18.2%.

The FTIR spectra of HG0, HSG10, HSG18, and HSG25 are presented in Figure 2. In the spectra of HG0 and HSG, the two absorption peaks at 1714/1717 and 1161/1163 cm^{-1} were attributed to the ester carbonyl (C═O) and C—O—C groups in HEMA and SBMA, respectively.[22] The spectra of HSG also displayed a characteristic peak at 1040 cm^{-1}, which resulted from the stretching vibrations of —SO_3 in the structure of SBMA.[24] However, the same peak was not observed in the spectra of HG0; this suggested the existence of SBMA in the network of HSGs. In addition, a band with a weak shoulder at 2940 cm^{-1} was assigned to the stretching vibrations of aliphatic —CH_2— and —CH_3 in the structure of HEMA and SBMA[10].

The surface morphologies of HG0 and HSG are shown in Figure 3. Large amounts of closed-type pores were formed in the structure of HG0, although this hydrogel had a highly porous architecture. However, a different structural morphology

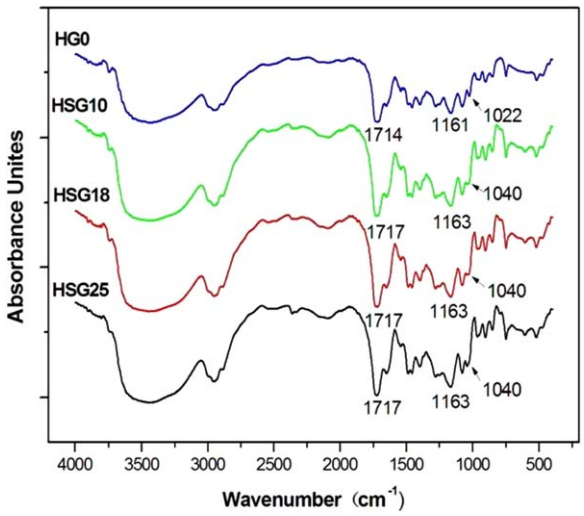

Figure 2. FTIR spectra of the PHEMA and HSGs. [Color figure can be viewed in the online issue, which is available at wileyonlinelibrary.com.]

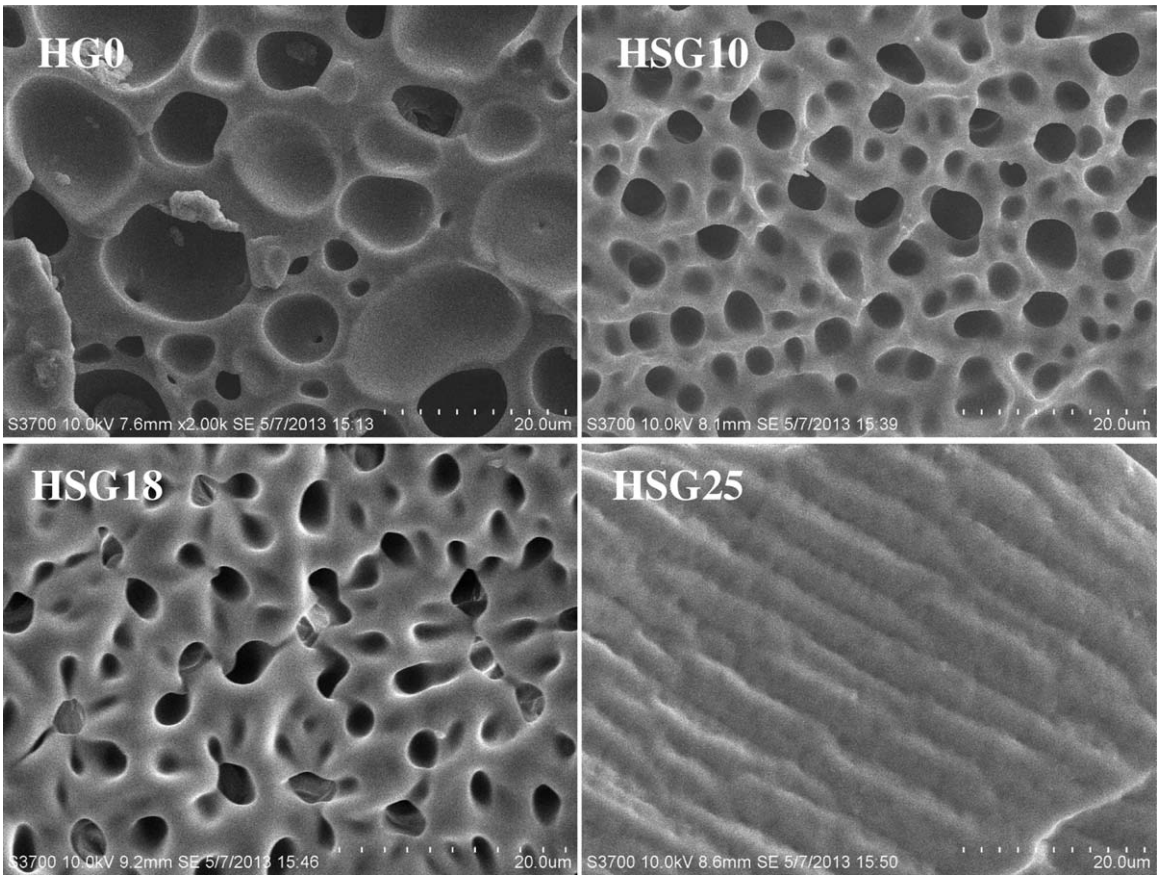

Figure 3. SEM micrographs of the PHEMA and HSGs.

was found in the HSG10 sample. The HSG10 exhibited a homogeneous microstructure with a relatively uniform pore size distribution, but the pore diameters of the HSG gradually decreased as the SBMA content increased, and a porous structure was not observed in the HSG25 sample. This was probably because the supporting force of the crosslinked networks increased with increasing feed ratios of SBMA and HEMA from HSG 10 to HSG25. This led to a decrease in the shrinking and a partial collapse of the networks during the freeze-drying process.[1] That is why the HSG exhibited a decreased pore size with increasing SBMA content. Thus, the porosity structure could be simply modulated by the feed ratios of the hydrogel.

Swelling Studies

The swelling behaviors of HG0 and HSG in deionized water are shown in Figure 4(a). The equilibrium swelling ratio (ESR), a critical parameter for estimating the properties of hydrogels, is usually affected by several factors, including the structural porosity, the hydrophilicity of the networks, and the crosslinking density.[10,25,26] As illustrated in Figure 3, the zwitterionic HSG exhibited decreased pore sizes in the network when the SBMA content was increased. Thus, the ESRs of the HSGs were expected to decrease with increasing SBMA content. However, the ESRs of the HSGs increased gradually with the SBMA content, and the porous HG0 showed a much lower ESR than those of the HSG [as shown in Figure 4(a)]. The low ESR of HG0 could be explained by the formation of intramolecular or intermolecular hydrogen bonds between the C═O and O─H bonds during gelation. These bonds made the polymeric chains bind together tightly and prevented these chains from expanding in distilled water and combining with water molecules.[22] In contrast, after the incorporation of the hydrophilic SBMA, the hydrophilicity of HSG was significantly improved; this made the gel network more easily hydrated and expanded regardless of the existence of intermolecular or intramolecular hydrogen bonds. The greater the SBMA content was, the higher the hydrophilicity of the gel network was. Therefore, an increase in the SBMA content in the hydrogel resulted in an increase in the SRs of the gels during the swelling process. This indicated that the swelling values of the zwitterionic HSG were mainly controlled by the hydrophilicity of the gel network, which strongly depended on the content of SBMA.

To further identify the effect of the SBMA content on the swelling behaviors of the hydrogels, the swelling values before equilibrium were fitted to the following empirical equation [eq. (1)]:[27]

$$\frac{W_t}{W_\infty} = kt^n \tag{1}$$

where W_t is the weight of the hydrogel at a certain time during the swelling process, W_∞ is the weight of the hydrogel after equilibrium, k is the characteristic constant involving structural and geometric characteristics of the hydrogel, and n is the characteristic diffusion exponent. A larger n indicates that more

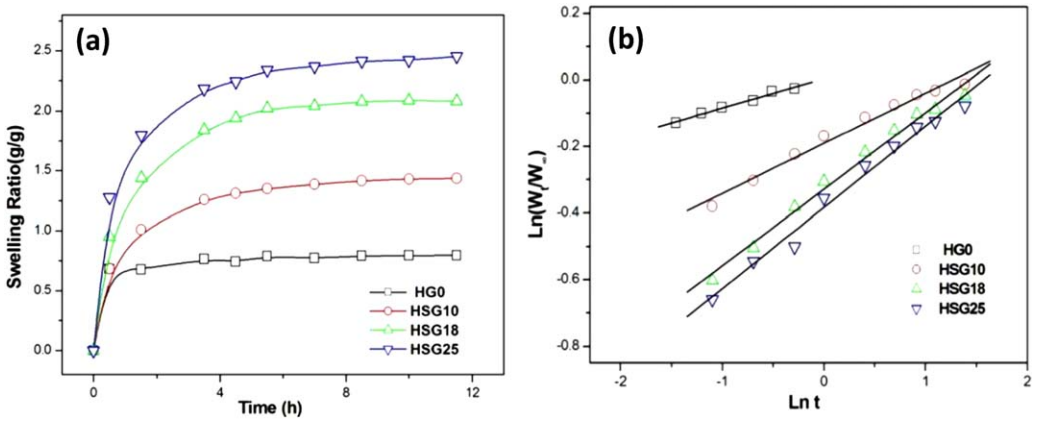

Figure 4. (a) Swelling behavior of PHEMA and HSG as a function of time. (b) Ln(W_t/W_∞) versus Ln t for the HG0 and HSGs. [Color figure can be viewed in the online issue, which is available at wileyonlinelibrary.com.]

water molecules penetrate into the gel network.[10] The fitted regression lines of the swelling data for all of the hydrogels are shown in Figure 4(b). n, k, and the correlation coefficient (R^2) values are summarized in Table II, from which we observed that HG0 showed the smallest n value of 0.116, whereas HSG exhibited an increased n with the SBMA content. This means that more water molecules diffused into HSG with increasing SBMA content; this implied that HSG25 had the higher ESR compared to the other HSGs with different weight percentages of SBMA. This was in accordance with our former discussion.

Mechanical Properties

The mechanical properties of HSG were evaluated with compression tests at 65% relative humidity. The results of these measurements are shown in Table III. We noted that the compression stresses of HSG increased from 74.5 to 319.8 KPa when the HEMA content was increased from 74.2 to 89.2% and HG0 showed the highest fracture stress of 735.8 KPa. We assumed that the mechanical strengths of HSG significantly depended on the HEMA/SBMA ratio. The different compression stresses of these gels mainly resulted from the following two reasons: (1) the formation of a dense gel network via chemical crosslinking and (2) the formation of hydrogen-bonding interactions caused by the hydroxyl group in HEMA; this was considered the primary factor in the enhancement of the mechanical properties of the HSGs.[6,12] Increasing the HEMA content in the gel made the gel absorb less water per polymer mass and led to a smaller water content in the gel matrix (as shown in Table III). In this case, the networks of the HSGs with higher HEMA amounts became denser.[6] Additionally, an increase in the content of HEMA was advantageous for improving the intermolecular interactions and led to the improvement of the mechanical strengths of the HSGs. Thus, the HEMA/SBMA ratios had a great influence on the mechanical strengths of the HSGs.

To further prove that H-bonding interactions from HEMA were responsible for the increased strengths of HSG, the pure PSBMA hydrogel (SG) was prepared with the same method. There were no H-bonding interactions existing in the SG because of a lack of the hydroxyl groups from HEMA. As shown in Table IV, SG with a similar water content to that of HSG25 sustained a compression stress of 13.5 KPa; this was about 5.5 times lower than that of HSG25. These results provide obvious evidence that the H-bonding interaction from HEMA played an important role in the enhancement of the mechanical properties of the gel.

Drug-Release Studies

TCHC was selected as the model drug and was loaded into the HSGs. It is believed that the average release amount is highly dependent on the loading efficiency of the hydrogel. Zhang et al.[28] and Wu et al.[29] reported that the drug-loading capacity was primarily dominated by the porous architecture of the hydrogel and that it increased with the porosity of the networks. In this study, SEM observations revealed that the porous microstructures for HSG gradually disappeared as the SBMA content was increased. We anticipated that the HSGs would exhibit decreased drug-loading efficiencies and average release amounts with increasing SBMA content. However, we found that the amount of

Table II. Results of the Fitting Parameters for the HG0 and HSGs

Hydrogel	SBMA (wt %)	k (h^{-1})	n	R^2
HG0	0	0.973	0.116	0.959
HSG10	10.8	0.848	0.140	0.969
HSG18	18.2	0.737	0.166	0.953
HSG25	25.8	0.682	0.244	0.983

Table III. Mechanical Properties of the Hydrogels

Hydrogel	SBMA (wt %)	HEMA (wt %)	Water content (wt %)	Stress (kPa)	Strain (%)
HG0	0	100	41.2	735.8	89.2
HSG10	10.8	89.2	59.2	319.8	87.8
HSG18	18.2	81.8	67.7	171.0	81.1
HSG25	25.8	74.2	71.5	74.5	80.1
SG	100	0	72.4	13.5	33.1

All of the hydrogel samples were synthesized with the same amount of the monomer (3.0 g).

Table IV. Fitting Parameters for the Release of TCHC from the Hydrogels

Hydrogel	SBMA (wt %)	K (min^{-1})	$D \times 10^4$ (cm^2/min)	R^2
HG0	0	0.0019	0.077	0.953
HSG10	10.8	0.004	0.162	0.973
HSG18	18.2	0.0025	0.101	0.962
HSG25	25.8	0.0062	0.252	0.988

k is the slope of the linear regression.

TCHC loaded into HG0, HSG10, HSG18, and HSG25 were 0.604, 0.885, 0.918, and 0.927 g, respectively; this implied that the drug-loading capacities increased with the SBMA content. In addition, as illustrated in Figure 5(a), the average release amounts of the HSGs also increased from 3.45 to 5.42 as the SBMA content was increased. This was different from previously reported results. This remarkable difference was attributed to the fact that the drug-loading efficiencies of these hydrogels relied not only on the porosity of the networks but also on the affinity effects between the drug molecules and the gel networks. TCHC is a hydrophilic drug molecule, which can be easily absorbed in the hydrophilic gel network during the drug-loading process because of the high affinity of the gel network with TCHC. As the content of SBMA was increased, the affinity effects between the TCHC and the networks also increased, although the pore sizes in the gel structure gradually decreased; this resulted in an increase in the loading efficiency of the TCHC per unit of polymer mass. During the process of drug release, a higher loading capacity allowed more TCHC molecules to spread into the medium and, hence, led to higher average release amounts of TCHC.

As shown in Figure 5(b), we observed that the time that the TCHC was released from HSG25 at 37°C was close to 300 min, whereas the TCHC release times of HSG18 and HG0 were approximately 780 and 1440 min, respectively. This suggested that HSG18 and HG0 were able to achieve sustained drug release for a longer time than HSG25. These differences may have been due to the following two reasons: (1) the lower hydrophilicity of the gel network with increasing HEMA content, which may have caused the slower swelling rate and, hence, weakened the driving force for drug release, and (2) the increased H-bonding interaction between the polymeric chains with increasing HEMA content, which probably produced a higher density region in the gel network to slow down the diffusion rate of TCHC and led to a prolonged drug-release time. However, we also noted that the TCHC release time of HSG10 was about 600 min, which was lower than that of HSG18. The decreased drug-release time may have been due to the increased porosity of HSG10. The structural porosity allowed water molecules to diffuse into the gel network and simultaneously allowed TCHC to move out of the hydrogel quickly; this made HSG10 achieve sustained TCHC release in a shorter period.

The drug-release rates of the HSGs were estimated according to the equation model [eq. (2)]. We converted this to eq. (3) by taking the first term in summation and using a logarithmic transformation:[30]

$$\frac{M_t}{M_\infty} = 1 - \frac{8}{\pi^2}\sum_{n=0}^{\infty}\frac{1}{(n+1)^2}\exp\left\{-\frac{(2n+1)^2 D\pi^2}{l^2}t\right\} \quad (2)$$

$$\ln\left(1-\frac{M_t}{M_\infty}\right) = \ln\frac{8}{\pi^2} - \frac{D\pi^2}{l^2}t \quad (3)$$

where M_∞ is the cumulative release of the drug at infinite time, l is the thickness of the gel disc, and D is the diffusion coefficient, which can be obtained from the slope t is the drug release time of the gel, $D\pi^2/l^2$ of the tread line by the plotting of $\ln(1 - M_t/M_\infty)$ against t. Particularly, the smaller D is, the slower the drug-release rate the gel is.

Figure 6 shows the fitted regression lines of the TCHC release data on the basis of eq. (3). The slope K, D, and R^2 of HSG are shown in Table IV. HSG25 exhibited the largest D of 25.2×10^{-4} cm^2/min, whereas the Ds of HSG18 and HG0 were 10.1×10^{-4} and 7.7×10^{-4} cm^2/min, respectively. This indicates that the TCHC release rates of HSG18 and HG0 were slower than that of HSG25. HSG10 showed a D of 16.2×10^{-4} cm^2/min; this was larger than that of HSG18. This confirmed our suggestion that HSG10 achieved sustained drug release for a longer time than HSG18.

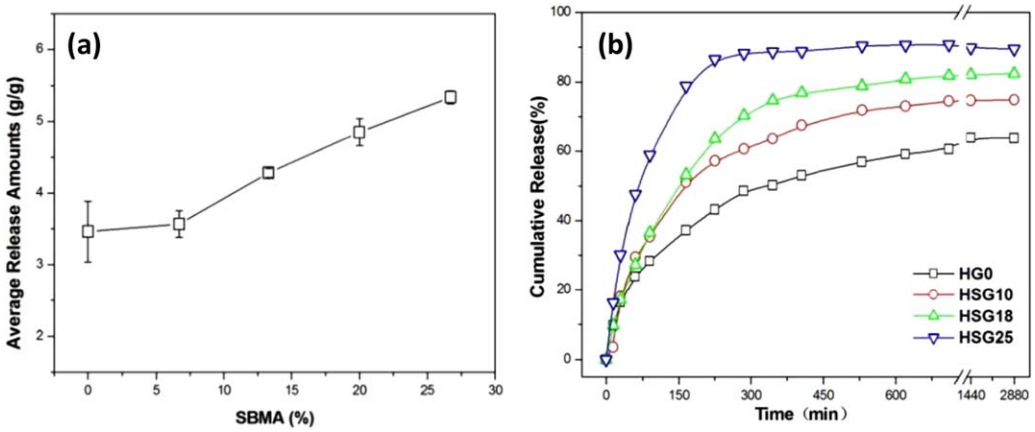

Figure 5. (a) Average amounts of TCHC released for HSGs with various SBMA contents. (b) Cumulative amounts of TCHC released from PHEMA and HSGs as a function of time at 37°C. [Color figure can be viewed in the online issue, which is available at wileyonlinelibrary.com.]

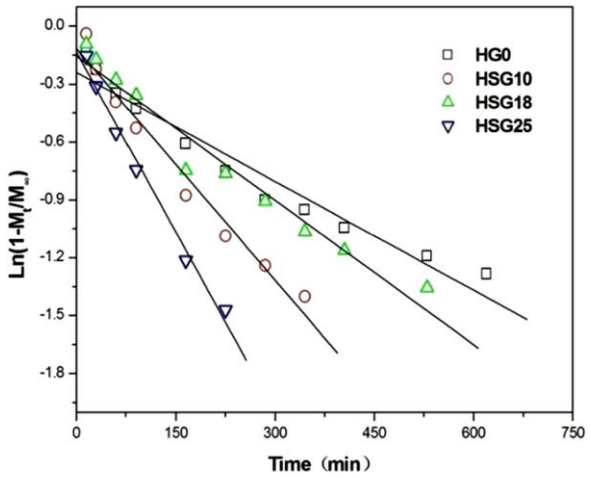

Figure 6. Plots of $\ln(1 - M_t/M_\infty)$ versus t for TCHC released from HG and HSGs. [Color figure can be viewed in the online issue, which is available at wileyonlinelibrary.com.]

Protein Adsorption Test

To evaluate the anti-protein-fouling abilities of the HSGs, HSG18 was selected as the model sample because of its enhanced mechanical strength, large average release amount, and long drug-release time. The protein adsorption of the fully swollen HSG18 was estimated by the exploitation of BSA as a model protein at 37°C. In addition, the amounts of protein absorbed on the HG0 and SG were also evaluated with the same method. As shown in Figure 7, we found that the BSA adsorption of HG0 was 112.5 $\mu g/cm^2$; this was about 11 times higher that of SG (10.3 $\mu g/cm^2$). This result was not in accordance with the previously reported research in which PHEMA and PSBMA coatings showed similar low-fouling properties.[24,31,32] This was probably because the protein adsorption on the hydrogel was decided not only by the hydrophilic properties of the gel surface but also by the porous structure.[33] We observed that the fully swollen HG0 possessed abundant pores with a spread of sizes. The porous microstructure allowed more BSA to penetrate into the hydrogel matrix and adhere to the effective pores, although the surface of HG0 showed highly hydrophilic properties to resist BSA adsorption; this led to a large amount of protein absorbed in HG0. This was in agreement with a previous report by Garrett et al.[33] In contrast, in the fully swollen state, SG presented a compact surface morphology with little pores because of the high water uptake in the gel network. Thus, it became extremely hard for the BSA molecules to penetrate into the SG network. On the other hand, the highly hydrophilic surface of SG could bind water molecules to form a strong hydration layer near the surface, and such hydration layer would produce a physical barrier to prevent protein adsorption. Therefore, little BSA was found to be absorbed on the SG.

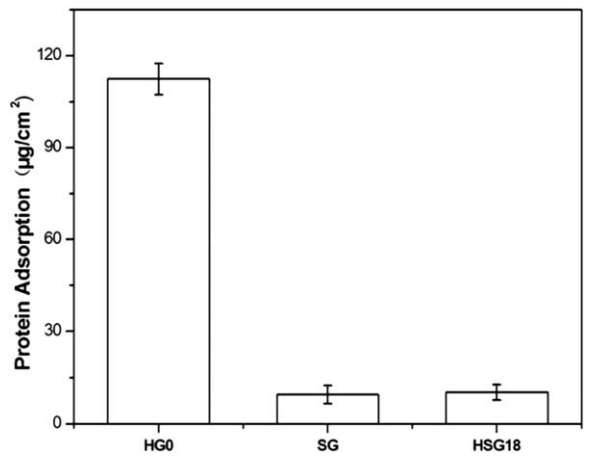

Figure 7. Adsorption of hydrogels in BSA solutions (1.0 mg/mL) for 24 h at 37°C.

As shown in Figure 7, the BSA adsorption on HSG18 was 11.4 $\mu g/cm^2$; this was close to that on SG. This indicated that HSG18 revealed the same excellent protein-resistance abilities as SG despite the incorporation of HEMA. This could be explained by the reason that HSG18 is a grafted hydrogel, and large amounts of flexible hydrophilic PSBMA chains existed on the gel surface, which could structurally separate from the gel backbone and form a strong hydration layer to resist protein adsorption.[4] Thus, HSG18 still retained good antifouling properties, even after the introduction of HEMA into the network.

CONCLUSIONS

Zwitterionic HSGs with different feed ratios were successfully prepared by the RAFT polymerization technique. Swelling studies showed that the ESR of the HSGs increased with the SBMA content because of the increased hydrophilicity of the gel network. As expected, the mechanical strengths of these grafted hydrogels were enhanced when the HEMA content was increased because of the formation of intermolecular interactions. The drug-release tests demonstrated that the average release amounts and the cumulative release of HSG were greatly dependent on the monomer feed ratios, and the TCHC release time of HSG was greatly prolonged by the adjustment of the feed ratios in the gels. Among all of the hydrogels, HSG18 exhibited an improved mechanical strength, long drug-release time, and good antifouling properties. This suggests that it has great potential for applications in drug-release devices.

ACKNOWLEDGMENTS

This work was financially supported by the National Science Foundation of China (contract grant number 21104021) and the Fundamental Research Funds for the Central Universities (contract grant number 2014ZM0057).

REFERENCES

1. Zhang, J.-T.; Bhat, R.; Jandt, K. D. *Acta Biomater.* **2009**, *5*, 488.
2. Zhang, J.-T.; Huang, S.-W.; Liu, J.; Zhuo, R.-X. *Macromol. Biosci.* **2005**, *5*, 192.
3. Zeng, R.; Xu, S.; Cai, Z.; Wen, X.; Pi, P.; Cheng, J. *Polym. Mater. Sci. Eng.* **2013**, *29*, 186.

4. Zeng, R.; Xu, S.; Cheng, J.; Cai, Z.; Pi, P.; Wen, X. *J. Appl. Polym. Sci.* **2014**, 131.
5. Zhang, X.-Z.; Wu, D.-Q.; Chu, C.-C. *Biomaterials* **2004**, *25*, 3793.
6. Gao, H.; Wang, N.; Hu, X.; Nan, W.; Han, Y.; Liu, W. *Macromol. Rapid Commun.* **2013**, *34*, 63.
7. Patil, N. S.; Dordick, J. S.; Rethwisch, D. G. *Biomaterials* **1996**, *17*, 2343.
8. Yin, L.; Fei, L.; Tang, C.; Yin, C. *Polym. Int.* **2007**, *56*, 1563.
9. Gong, J. P.; Katsuyama, Y.; Kurokawa, T.; Osada, Y. *Adv. Mater.* **2003**, *15*, 1155.
10. Xiang, Y.; Peng, Z.; Chen, D. *Eur. Polym. J.* **2006**, *42*, 2125.
11. Tanaka, Y.; Gong, J. P.; Osada, Y. *Prog. Polym. Sci.* **2005**, *30*, 1.
12. Tang, L.; Liu, W.; Liu, G. *Adv. Mater.* **2010**, *22*, 2652.
13. Bostan, L.; Trunfio-Sfarghiu, A. M.; Verestiuc, L.; Popa, M. I.; Munteanu, F.; Rieu, J. P.; Berthier, Y. *Tribol. Int.* **2012**, *46*, 215.
14. Yusa, S.-I.; Fukuda, K.; Yamamoto, T.; Ishihara, K.; Morishima, Y. *Biomacromolecules* **2005**, *6*, 663.
15. Xu, X.; Smith, A. E.; Kirkland, S. E.; McCormick, C. L. *Macromolecules* **2008**, *41*, 8429.
16. Xu, S.; Zeng, R.; Cheng, J.; Cai, Z.; Wen, X.; Pi, P. *J. Appl. Polym. Sci.* **2014**, 131.
17. Liu, Q.; Zhang, P.; Qing, A.; Lan, Y.; Lu, M. *Polymer* **2006**, *47*, 2330.
18. Liu, Q.; Zhang, P.; Lu, M. *J. Polym. Sci. Part A: Polym. Chem.* **2005**, *43*, 2615.
19. Wang, R.; McCormick, C. L.; Lowe, A. B. *Macromolecules* **2005**, *38*, 9518.
20. Carr, L. R.; Zhou, Y.; Krause, J. E.; Xue, H.; Jiang, S. *Biomaterials* **2011**, *32*, 6893.
21. Li, Q.; Bi, Q.-Y.; Zhou, B.; Wang, X.-L. *Appl. Surf. Sci.* **2012**, *258*, 4707.
22. Guürdağ, G. L.; Kurtulus¸, B. *Ind. Eng. Chem. Res.* **2010**, *49*, 12675.
23. Bune, Y. V.; Barabanova, A. I.; Bogachev, Y. S.; Gromov, V. F. *Eur. Polym. J.* **1997**, *33*, 1313.
24. Chiang, Y.-C.; Chang, Y.; Higuchi, A.; Chen, W.-Y.; Ruaan, R.-C. *J. Membr. Sci.* **2009**, *339*, 151.
25. Kim, J. H.; Lee, S. B.; Kim, S. J.; Lee, Y. M. *Polymer* **2002**, *43*, 7549.
26. Singh, B.; Pal, L. *Eur. Polym. J.* **2008**, *44*, 3222.
27. Jin, X.; Hsieh, Y.-L. *Polymer* **2005**, *46*, 5149.
28. Zhang, J.-T.; Petersen, S.; Thunga, M.; Leipold, E.; Weidisch, R.; Liu, X.; Fahr, A.; Jandt, K. D. *Acta Biomater* **2010**, *6*, 1297.
29. Wu, W.; Liu, J.; Cao, S.; Tan, H.; Li, J.; Xu, F.; Zhang, X. *Int. J. Pharm.* **2011**, *416*, 104.
30. Pekcan, Ö.; Erdoğan, M. *Eur. Polym. J.* **2002**, *38*, 1105.
31. Mrabet, B.; Nguyen, M. N.; Majbri, A.; Mahouche, S.; Turmine, M.; Bakhrouf, A.; Chehimi, M. M. *Surf. Sci.* **2009**, *603*, 2422.
32. Zhang, Z.; Chen, S.; Chang, Y.; Jiang, S. *J. Phys. Chem. B* **2006**, *110*, 10799.
33. Garrett, Q.; Chatelier, R. C.; Griesser, H. J.; Milthorpe, B. K. *Biomaterials* **1998**, *19*, 2175.